

An Ultrawideband Planar Elliptical Slotted Patch Antenna without any Matching Liquid for Biomedical Application

Fnu Mansoor, Saeed I. Latif*

Department of Electrical and Computer Engineering
University of South Alabama
150 Jaguar Dr., SHBC 4122, Mobile, AL 36688, USA
Emails: mansoor7696@gmail.com, slatif@southalabama.edu

*Corresponding author

Received: October 06, 2018

Accepted: November 07, 2019

Published: June 30, 2020

Abstract: The design and analysis of a planar ultra-wideband elliptical slotted patch antenna for application in breast microwave radar system is presented in this paper. It is modelled in front of a breast phantom of cylindrical shape. No matching liquid is used in this model. A novel partial ground plane with protrusions on two sides is used for achieving good matching without any coupling medium. For effective signal penetration, a low frequency band of operation is selected. The antenna has a wide impedance bandwidth operating from around 1.8 GHz to 6.9 GHz or higher. A parametric study is conducted to understand the effects of important parameters on the antenna performance and to develop some design guidelines. The fabricated prototype was tested in the presence of a breast phantom. The transmission response of the antenna was also measured, which shows reduced transmission loss compared to a previous study since the antenna is in the air. The measured results are in good agreement with simulated data. This antenna can be used in a microwave imaging system for radar based breast cancer detection, where wide impedance bandwidth is required.

Keywords: Ultra-wideband antenna (UWB), Elliptical slotted patch, Matching material, Printed antennas, Wide impedance bandwidth.

Introduction

Microwave signals can penetrate electromagnetically opaque and non-conducting materials. This allows embedded defects and/or buried objects to be non-destructively detected by determining the contrasting dielectric properties of the defect and the surrounding structure [7]. This concept is used for microwave imaging of human breast for breast cancer detection. Microwave Imaging has been proposed as an alternative to X-Ray mammography or Magnetic Resonance Imaging (MRI) due to its non-ionizing radiation [13]. Mammogram technique uses ionizing radiation and has false positive rates between 60%-70% and false negative rates of over 15% [14]. A false positive is an error in test result which incorrectly indicates that a particular condition or attribute is present. Similarly, a false negative is an error in test result which indicates that a particular condition or attribute is absent, whereas it is actually present. On the other hand, MRI is expensive and not portable as a mass screening tool. Ultrasound imaging requires skilful practitioner and has high false positive rates [8]. Microwave imaging technology has the potential to be a compact and portable system for use as a mass screening tool, especially in remote areas. In this technique, the difference in dielectric properties between malignant tumors and the surrounding normal breast tissue is detected using microwave antennas, where one antenna illuminates the breast and the scattered signal is detected by sensors or other antennas in the system [1, 3, 6]. Specifically, for radar-based microwave imaging, wideband antennas operating in the lower frequency spectrum is desired [5, 9, 11].

Wideband water-filled double-ridged horn antennas [11], stacked patch antennas and slot antennas [9], balanced antipodal Vivaldi antennas [4], double-ridged horn antennas in canola oil [10] and printed planar monopole antennas [12] are proposed for this imaging approach. In all these designs, a matching medium is used to reduce the reflection from the breast tissue. Three tapered slot antennas are presented in [15] to cover various sub-bands within 3 GHz to 10 GHz bandwidth, which are arranged in an array without any matching liquid for an ultra-wideband microwave imaging System. In this paper, the design of a single planar ultra-wideband (UWB) elliptical monopole antenna operating at much lower frequencies is presented for application in radar-based breast imaging where no matching material is used.

The proposed UWB elliptical slotted patch antenna is designed in front of a cylindrical breast phantom required for this application. The breast phantom is modeled with fatty and normal tissues with a skin layer over it. In [12], a UWB elliptical monopole antenna immersed in a matching liquid is presented. In our present design, a slot is introduced in the monopole elliptical patch for miniaturization and no immersing or coupling medium is used. The antenna is in the free-space with a small separation from the phantom, and operates in the lower frequency band (around 1.8-6.9 GHz) chosen for efficient signal penetration. If no matching material is needed, this will reduce the system complexity greatly, and a compact system can be achievable. Since the signal attenuation is higher in any matching medium other than air, less transmission loss is expected in the proposed model. The detailed simulation and modeling is described in the next section, followed by results and discussion. Measurements are conducted and results are presented. Conclusions are drawn at the end.

Design methods and results

The geometry of the ultra-wideband elliptical ring-patch antenna is shown in Fig. 1. It is etched on one side of Rogers RT/duroid 5880 substrate with permittivity, $\epsilon_r = 2.2$, and thickness, $h = 0.79$ mm. The size of the substrate is: length, $A = 60$ mm, and width, $B = 35.8$ mm. The elliptical slotted patch is excited by a $50\text{-}\Omega$ feed line having width, $F = 2.0$ mm. The elliptical patch's major axis length is: $b = 45$ mm, which is quarter-wave in length at the lowest frequency. Its minor axis is: $a = 31$ mm. To achieve miniaturization, a small metal portion is removed from the center of the elliptical patch creating a slot on it. This removal increases the current flow path reducing the low frequency further [2]. The slot has major and minor axes dimensions as follows: $b_1 = 9$ mm and $a_1 = 6.2$ mm, respectively. On the other side of the substrate, there is a partial ground plane with length, $Gr_L = 14$ mm at the center. It has two protrusions on either side having a height, $E_L = 2.5$ mm. These protrusions are formed by cutting an ellipse having a semi-minor axis of 2.5 mm on a rectangle. It is found by parametric study that, along with other parameters, these protrusions help in matching the antenna to the target so that no coupling medium is needed in the system. Other shapes of the ground plane, e.g. oval shaped ground plane was studied. However, this protrusion gives the best matching for this setup. The ground plane and the elliptical slotted patch are separated by a distance, $s = 0.5$ mm at their closest point in the middle. These antenna parameters are listed in Table 1. The antenna is placed in front of a breast phantom, as shown in Fig. 2, where no matching material is used between the antenna and the breast phantom. The cylindrical breast phantom has a height of 100 mm, and a radius of 90 mm. The phantom has a 2 mm thick skin layer with permittivity, $\epsilon_r = 36$, and is placed $D = 50$ mm away from the antenna, as shown in Fig. 2. The phantom is filled with fatty breast tissue, having permittivity, $\epsilon_r = 6$. The materials used have their properties available in the CST Microwave Studio Material Library. All simulations are conducted in CST Microwave Studio. The antenna parameters are judiciously selected and optimized so that matching can be achieved without the need of a coupling medium which is typical in most of the designs available in the literature.

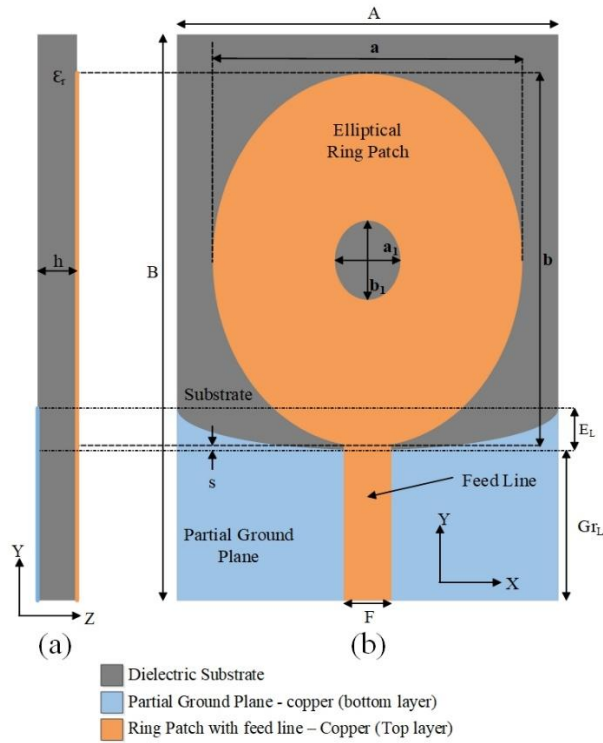


Fig. 1 Geometry of the ultra-wideband planar elliptical monopole ring-patch antenna: (a) side view; (b) top view.

Table 1. Optimized antenna parameters

Parameters	Values, (mm)
Length of the substrate (B)	60
Width of the substrate (A)	35.8
Thickness of the substrate (h)	0.79
Substrate permittivity (ϵ_r)	2.2
Minor axis of the patch (a)	31
Major axis of the patch (b)	45
Elliptical slot minor axis (a_1)	6.2
Elliptical slot major axis (b_1)	9
Distance between the ring patch and the ground (s)	0.5
Protrusions on either end of the ground (E_L)	2.5
Feed width (F)	2.0
Ground plane length (Gr_L)	14

Parametric study

A detailed parametric study is conducted to understand the effect of varying several parameters on the reflection coefficient of this antenna, as well as, to develop some design guidelines. The slotted elliptical patch dimensions are responsible for the operating frequency of the antenna. Other parameters are optimized for obtaining impedance matching of the antenna without any coupling medium. For brevity, only three critical parameters that provide wide impedance bandwidth as well as good matching are discussed here. The study is conducted keeping all parameters fixed as mentioned in Table 1, while varying only one parameter at a time.

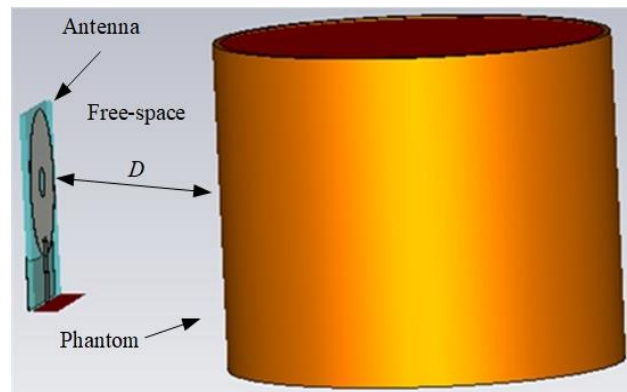


Fig. 2 Simulation setup for the design of the proposed antenna: the UWB elliptical monopole slotted patch antenna is in front of a humanoid cylindrical Breast phantom. The antenna is in the air and 50 mm away from the phantom.

Varying the ground plane length (Gr_L)

In this design, no matching liquid is used in the model and the matching is achieved by effectively adjusting various antenna parameters. Among several parameters, a very important one is the ground plane length Gr_L . The effect of its variation from 12.5 mm to 15.5 mm on the reflection coefficient is shown in Fig. 3. This parameter significantly affects the reflection coefficient in the mid-band: as Gr_L increases, the reflection coefficient increases at mid-band frequencies. On the other hand, for a smaller Gr_L value, the impedance bandwidth decreases due to higher reflection coefficients at higher frequencies. With $Gr_L = 14$ mm, the antenna shows a good impedance matching for a large frequency band.

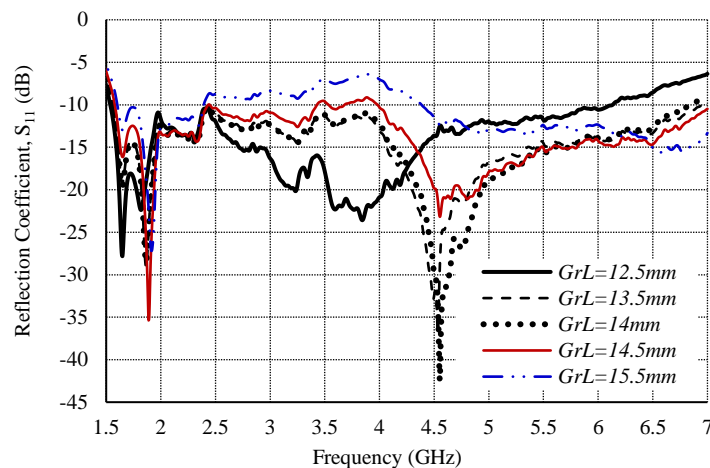


Fig. 3 Simulated return loss obtained by varying the ground plane length Gr_L

Varying protrusions on either end of the ground plane (E_L)

The effects of varying protrusions (E_L) on either side of the ground plane on reflection coefficients are shown in Fig. 4. This parameter is varied from 1.3 mm to 2.5 mm. It is noticed that this parameter mostly influences the reflection coefficient in the mid-band: as E_L increases, the reflection is higher at mid-band frequencies. At the same time, the matching degrades at higher frequencies. In fact, for an optimum Gr_L value, this parameter provides good impedance in the middle frequency allowing wide bandwidth operation.

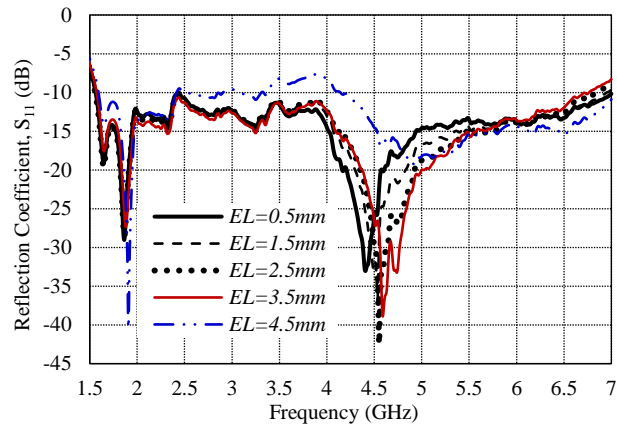


Fig. 4 Simulated return loss obtained by varying protrusions on either end of the ground plane (E_L)

Varying spacing between patch and ground (s)

The effect of varying the distance between the patch and the ground (s) on the reflection coefficient of this antenna is shown in Fig. 5. The following s values are chosen for this parametric study: -0.5 mm, -0.2 mm, 0.3 mm, 0.5 mm, and 0.8 mm. A negative value of s specifies the overlapping of the ground plane and the elliptical slotted patch. While a large overlap affects negatively the reflection coefficient of the antenna at mid-frequencies, a large value of s , i.e., a large spacing causes poor reflection coefficient at higher frequencies. With $s = 0.5$ mm, the impedance bandwidth achieved from this antenna is 5.4 GHz or 126% (from 1.6 GHz to 7 GHz).

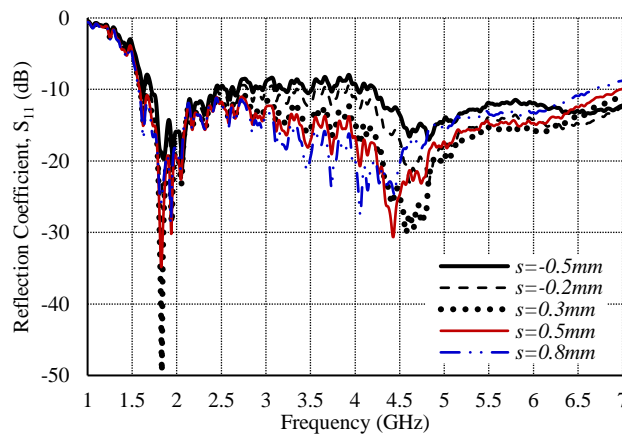
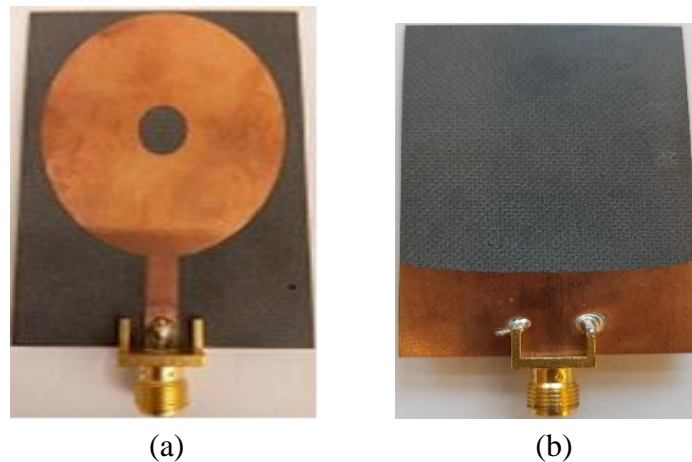


Fig. 5 Simulated return loss obtained by varying the spacing between the patch and the ground plane (s)

Measurement results

Based on the parametric study, antenna parameters are optimized to achieve impedance matching with the breast phantom without any matching liquid. Several optimized antenna prototypes were fabricated and tested at the Applied Electromagnetics Research Lab (AERL) at the University of South Alabama. The top and bottom sides of a fabricated prototype are shown in Fig. 6.

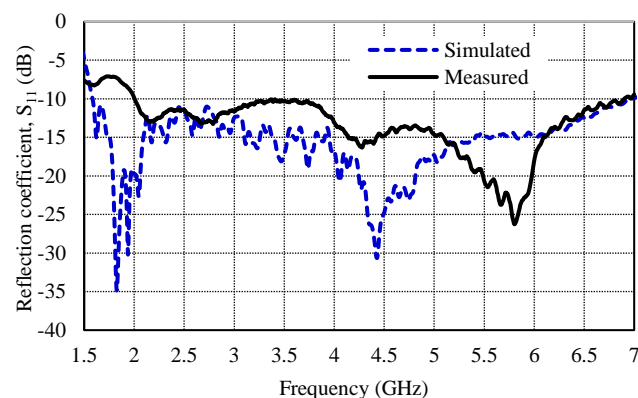


(a) (b)
Fig. 6 Fabricated ultra-wideband printed antenna:
(a) top view; (b) bottom view.

The measurement setup for measuring reflection coefficient is presented in Fig. 7(a). The optimized antenna exhibits a simulated $S_{11} \approx -10$ dB bandwidth from 1.58 GHz to 6.98 GHz (about 126.1%) as shown in Fig. 7(b), for the parameters listed in Table 1.



(a)

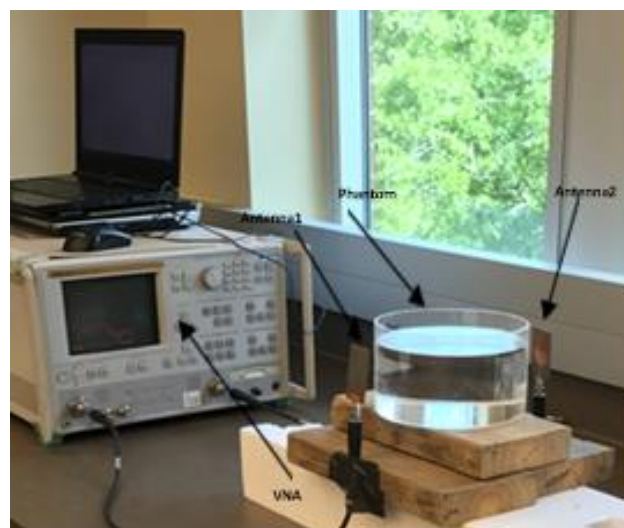


(b)

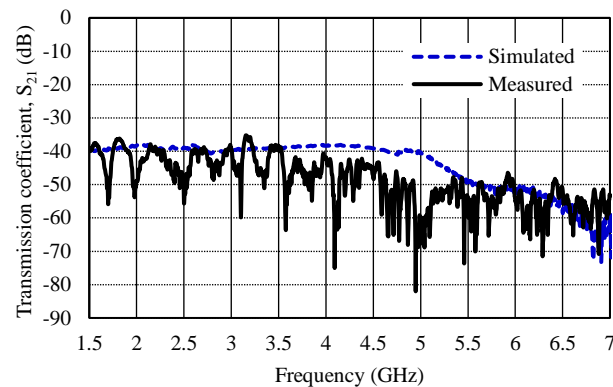
Fig. 7 Experimental setup for measuring reflection coefficient (S_{11}) and the comparison of simulated and measured reflection coefficient with frequency of the antenna:
(a) experimental setup; (b) reflection coefficient comparison.

This frequency range is suitable for breast imaging, as it provides necessary signal penetration into the breast. The measurement of the fabricated antenna was conducted on an Anritsu 37369A Vector Network Analyzer, and the measured reflection coefficient in front of a phantom is compared in the same graph in Fig. 7(b). The phantom was made of a container filled with glycerin, which has permittivity of 9 and conductivity of 0.4 S/m. The container height is 90 mm and its radius is 100 mm, with wall thickness of 2 mm. Measured $S_{11} \approx -10$ dB bandwidth of this antenna is 5 GHz or 112% (from 1.95 GHz to 6.9 GHz). A difference in measured and simulated reflection coefficients at lower frequencies can be noticed, which can be attributed to fabrication errors and discrepancies in permittivities of materials used in simulation and measurement, such as glycerin. Other differences, such as, skin layer, container wall thickness, etc, might also have contributed to that. Nevertheless, the measured S_{11} response was below -7 dB for a large frequency spectrum ranging from 1.5 GHz to 7 GHz. Since the antenna is almost in the near field, radiation patterns were not measured, rather the transmission coefficient, or S_{21} , was recorded, which is an important parameter in radar based microwave imaging. A low value of S_{21} indicates effective signal penetration that fosters the scattering of the signal from the target.

The experimental setup shown in Fig. 8(a) was used to conduct this measurement, where two antennas were placed 180° apart separated by the phantom. Measured transmission coefficient is compared with simulated ones in Fig. 8(b). Like in the case of reflection coefficient, a small difference in measured and simulated results at middle frequencies can be noticed, which can be attributed to the same reason, as mentioned before. In general, both simulated and measured results have the same trend. It can be observed that at low frequencies, the transmission coefficient (S_{21}) is around -40 dB. However, at high frequencies its average value is about -60 dB. This shows a significant improvement in the transmission performance of a UWB antenna without a reflector, compared to that presented in [12] with a UWB planar antenna backed by a reflector, where S_{21} is around -50 dB from 1 GHz to 4 GHz, and -70 dB at higher frequencies. The improved S_{21} is critical for breast imaging to obtain higher sensitivity with better signal-to-noise ratio.



(a)



(b)

Fig. 8 Experimental setup for measuring transmission coefficient (S_{21}), and measured transmission coefficient of the antenna:
(a) experimental setup; (b) transmission coefficient comparison.

Conclusion

A UWB elliptical slotted patch antenna in the presence of a breast phantom is presented in this paper. The effects on the reflection and transmission coefficients of the antenna are studied when placed in front of a breast phantom but without any matching medium. It has been shown that a good matching can be achieved by selecting antenna parameters judiciously without using any coupling liquid. The antenna demonstrates wide impedance bandwidth from 1.8 GHz to 7.0 GHz. The measured results are in reasonably good agreement with simulations. Since no matching liquid was used, an improved transmission response is achieved. This antenna can be used in a breast imaging system based on radar technology to detect early stage breast cancer detection, where wide impedance bandwidth is required.

Acknowledgments

The authors would like to acknowledge the grant support provided by the National Institutes of Health (NIH) – CCTS Partner Network Multidisciplinary Pilot Program and the University of South Alabama Faculty Development Council (USAFDC) for partially funding this project.

References

1. Abbak M., M. Cayoren, I. Akduman (2014). Microwave Breast Phantom Measurements with a Cavity-backed Vivaldi Antenna, *IET Microwaves, Antennas & Propagation*, 8, 1127-1133.
2. Bafrooei P. M., L. Shafai (1999). Characteristics of Single- and Double-layer Microstrip Square Ring Antennas, *IEEE Transactions on Antennas and Propagation*, 47, 1633-1639.
3. Bond E. J., X. Li, S. C. Hagness, B. D. Van Veen (2003). Microwave Imaging via Space-Time Beamforming for Early Detection of Breast Cancer, *IEEE Transactions on Antennas and Propagation*, 51, 1690-1705.
4. Bourqui J., M. Okoniewski, E. C. Fear (2010). Balanced Antipodal Vivaldi Antenna with Dielectric Director for Near-field Microwave Imaging, *IEEE Transactions on Antennas and Propagation*, 58, 2318-2326.
5. Byrne D., M. Sarafianou, I. J. Craddock (2016). Compound Radar Approach for Breast Imaging, *IEEE Transactions on Biomedical Engineering*, 64, 40-51.

6. Chiappe M., G. L. Gragnani (2006). Vivaldi Antennas for Microwave Imaging: Theoretical Analysis and Design Considerations, *IEEE Transactions on Instrumentation and Measurement*, 55, 1885-1891.
7. Daniels D. (2004). *Ground Penetrating Radar*, IEE Press, London, UK.
8. Flory D., M. W. Fuchsjaeger, C. F. Weisman, T. H. Helbich (2009). Advances in Breast Imaging: A Dilemma or Progress?, *Minimally Invasive Breast Biopsies*, 173, 159-181.
9. Gibbins D., M. Klemm, I. J. Craddock, J. A. Leendertz, A. Preece, R. Benjamin (2010). A Comparison of a Wide-slot and a Stacked Patch Antenna for the Purpose of Breast Cancer Detection, *IEEE Transactions on Antennas and Propagation*, 58, 665-674.
10. Latif S. I., D. Flores-Tapia, D. R. Herrera, M. S. Nepote, S. Pistorius, L. Shafai (2015). A Directional Antenna in a Matching Liquid for Microwave Radar Imaging, *International Journal of Antennas and Propagation*, Article ID 751739, <https://doi.org/10.1155/2015/751739>.
11. Latif S. I., D. Flores-Tapia, S. Pistorius, L. Shafai (2015). Design and Performance Analysis of the Miniaturised Water-filled Double-ridged Horn Antenna for Active Microwave Imaging Applications, *IET Microwaves, Antennas & Propagation*, 9, 1173-1178.
12. Latif S. I., S. Pistorius, L. Shafai, D. Flores-Tapia (2014). A Planar Ultrawideband Elliptical Monopole Antenna with Reflector for Breast Microwave Imaging, *Microwave and Optical Technology Letters*, 56, 808-813.
13. Nikolova N. K. (2014). Microwave Imaging for Breast Cancer, *IEEE Microwave Magazine*, 12, 78-94.
14. Patlak M., S. J. Nass, I. C. Henderson, J. C. Lashof (2001). *Mammography and Beyond*, National Academy of Press, Washington, D.C., USA.
15. Wang Y., A. M. Abbosh, B. Henin, P. T. Nguyen (2014). Synthetic Bandwidth Radar for Ultra-wideband Microwave Imaging Systems, *IEEE Transactions on Antennas and Propagation*, 62, 698-705.

Fnu Mansoor, M.Sc.

E-mail: mansoor7696@gmail.com



Fnu Mansoor is a RF Engineer at Amdocs, USA. He has a M.Sc. degree in Electrical and Computer Engineering from University of South Alabama, USA. His research interests include antennas and sensors for biomedical devices, antenna arrays for 4G/5G wireless systems, etc.

Assoc. Prof. Saeed I. Latif
E-mail: slatif@southalabama.edu



Dr. Saeed I. Latif is an Associate Professor with the Department of Electrical and Computer Engineering at the University of South Alabama, USA. He is a Senior Member of IEEE and has authored/co-authored 2 book chapters and 80+ journal and conference articles. He is the 2020 USA College of Engineering ‘Excellence in Research Award’ recipient and received IEEE Antennas and Propagation Edward E. Altshuler Best Paper Award in 2014. His research interests include antenna design/analysis for mobile and satellite communications, biomedical application of antennas, frequency selective surfaces, millimeter wave antennas for 5G wireless systems, and engineered conductors.



© 2020 by the authors. Licensee Institute of Biophysics and Biomedical Engineering, Bulgarian Academy of Sciences. This article is an open access article distributed under the terms and conditions of the Creative Commons Attribution (CC BY) license (<http://creativecommons.org/licenses/by/4.0/>).